

Early-stage suppression of Cu (001) oxidation

J. A. Eastman,^{a)} P. H. Fuoss, L. E. Rehn, P. M. Baldo, G.-W. Zhou,
D. D. Fong, and L. J. Thompson

Materials Science Division, Argonne National Laboratory, Argonne, Illinois 60439

(Received 25 February 2005; accepted 14 June 2005; published online 27 July 2005)

In situ synchrotron x-ray studies of the early-stage oxidation behavior of Cu (001) reveal that for Cu₂O nanoislands, the Cu–Cu₂O equilibrium phase boundary is shifted to larger oxygen partial pressure (p_{O_2}) by many orders of magnitude relative to bulk Cu₂O. Real-time scattering measurements find that an ordered surface structure appears with increasing p_{O_2} , followed by the nucleation of epitaxial Cu₂O nanoislands. By adjusting the p_{O_2} , it is possible to reversibly grow or shrink these islands and accurately determine the equilibrium phase boundary. These observations provide insight into the general stability of oxide nanoclusters grown by various techniques. © 2005 American Institute of Physics. [DOI: 10.1063/1.2005396]

Although extensive interest in metal and metallic alloy oxidation behavior has existed for decades, there is still surprisingly little known about the atomic-level and mesoscopic processes that take place between the initial adsorption of oxygen on a clean metal surface, and the formation of a continuous, macroscopically thick oxide layer. Early-stage oxidation theories such as that of Cabrera and Mott¹ are commonly cited and employed; however they suffer serious deficiencies. For example, Yang *et al.*² recently pointed out that while the Cabrera–Mott theory assumes uniform layer-by-layer growth of an oxide phase starting with a continuous monolayer, several reports³ have indicated that initial oxidation of many metals actually occurs by nucleation, growth, and coalescence of islands. Other important aspects of initial oxidation behavior, such as possible size-dependent changes in phase equilibria, are also unexplored and provide motivation for new studies.

Understanding and controlling early-stage oxidation behavior is important for a wide range of current and envisioned applications. In forming tunnel junctions for magnetic random-access memories (MRAM),⁴ controlled formation of a stable, continuous thin oxide layer is desired. In other applications, suppression of oxidation is vital. For example, Cu is of interest as an electrode material in strategies for integrating high-dielectric-constant oxide materials such as (Ba_xSr_{1-x})TiO₃ into Si-based electronic devices.⁵ However, oxidation of the thin film Cu electrodes during growth of the dielectric materials in an oxygen partial pressure must be avoided. While the conditions under which stable bulk Cu-oxide phases form are well known, the behavior may be quite different during initial oxidation, where oxide nanoislands nucleate and grow. In the present study, we have used *in situ* synchrotron x-ray techniques to determine conditions for phase equilibria between Cu₂O nanoislands and the Cu (001) surface.

A key barrier holding back progress in manipulating early-stage oxidation processes has been the scarcity of structural, chemical, and kinetic information obtained *in situ*, during oxidation. While recent *in situ* transmission electron microscopy (TEM) studies have provided valuable informa-

tion on temperature-dependent oxide island morphology and growth kinetics during oxidation of single-crystal metal thin films, particularly Cu (001)^{2,6} and (110),⁷ the range of p_{O_2} typically accessible in existing environmental TEMs is insufficient for probing oxide phase equilibria. The present study uses synchrotron x-ray scattering techniques that are particularly well-suited for *in situ* studies over a wide range of p_{O_2} and temperature.

This study used a controlled environment system recently constructed for use at the Advanced Photon Source. A high temperature (≤ 1000 °C) oxidizing/reducing environment is created within a quartz-walled chamber mounted on a six-circle diffractometer (Beamline 12-ID-B). The temperature was monitored and controlled using a thermocouple in contact with the sample heater. The thermocouple readings are calibrated by comparing measured and known lattice parameter values for materials with well-characterized thermal expansion behavior.

The chamber is evacuated to a base pressure of $\sim 1 \times 10^{-7}$ Torr using a compact turbomolecular pump backed by an oil-free scroll pump. Oxidizing and reducing environments are created by mixing purified gases

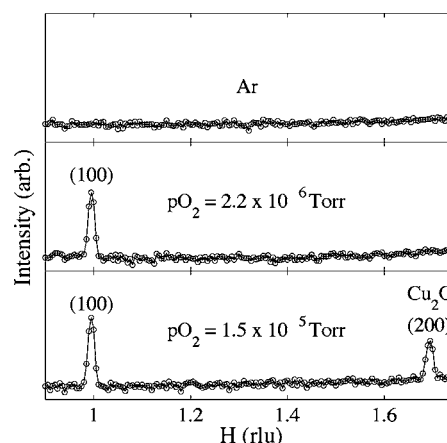


FIG. 1. In-plane (H00) scans at 475 °C of the same sample in varying p_{O_2} (the H values are shown in reciprocal lattice units referenced to Cu). After exposure of the initially clean surface to $p_{O_2} = 2.2 \times 10^{-6}$ Torr, a peak appears at (100) due to the formation of an ordered $c(2 \times 2)$ surface structure. Raising the p_{O_2} to 1.5×10^{-5} Torr results in oxidation to form Cu₂O nanoislands that coexist with the $c(2 \times 2)$ structure.

^{a)} Author to whom correspondence should be addressed; electronic mail: jeastman@anl.gov

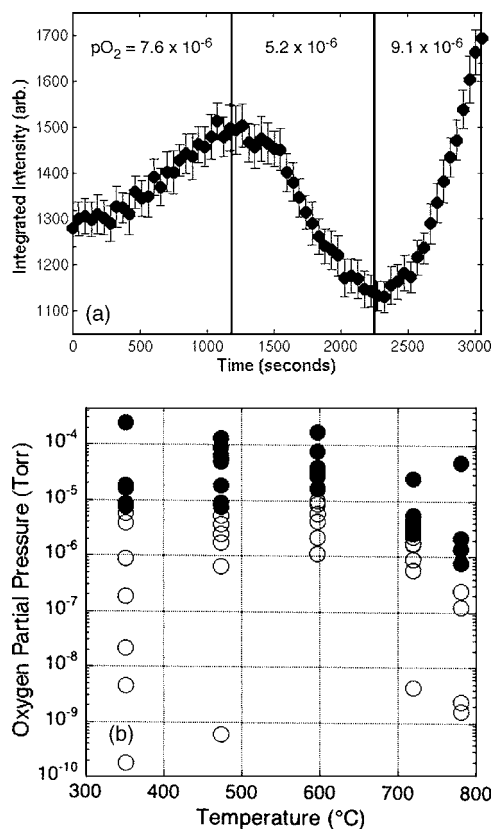


FIG. 2. (a) Measurements of the integrated intensity of the Cu_2O (200) Bragg reflection in varying $p\text{O}_2$ revealed that small changes in $p\text{O}_2$ could result in a change from oxidation to reduction (or vice versa). The temperature during the measurements shown was 475°C . (b) by measuring the $p\text{O}_2$ at which behavior switched from oxidation (closed symbols) to reduction (open symbols), the Cu– Cu_2O phase boundary was determined at several temperatures.

(Ar, O_2 , CO, CO_2 , H_2) via a series of mass-flow controllers and introducing this mixture through a leak valve that controls the chamber pressure. Oxygen partial pressures as low as 1×10^{-11} Torr can be achieved. A residual gas analyzer is used for monitoring the sample environment.

Epitaxial (001) Cu thin film samples with thicknesses of 110–200 nm were grown by electron-beam evaporation onto SrTiO_3 single crystal (001) substrates. After mounting in the environmental chamber, samples were annealed typically for 1 h at $\sim 840^\circ\text{C}$ in 5×10^{-4} Torr of Ar-2% H_2 and then were cooled to the desired temperature for oxidation studies. This treatment removed any native oxide and improved the Cu crystal quality, resulting in typical film rocking curves with $\text{FWHM} \leq 0.1^\circ$. A grazing-incidence diffraction geometry was used to monitor in-plane periodicities, while high-angle diffraction was used to probe reciprocal space in the direction normal to the sample surface.

At all temperatures investigated in this study, samples exposed to vacuum, Ar, or Ar-2% H_2 environments exhibited the normal diffraction peaks expected for a face-centered cubic (fcc) crystal. Exposure to a low $p\text{O}_2$, achieved by mixing O_2 and Ar, invariably resulted in the formation of additional sharp reflections at normally forbidden mixed-indices locations such as (100) (see Fig. 1). These reflections are associated with an oxygen-stabilized ordered surface structure having $c(2 \times 2)$ symmetry. This surface structure persisted even after increasing the $p\text{O}_2$ to nucleate and grow Cu_2O islands, consistent with a previously reported TEM observation that

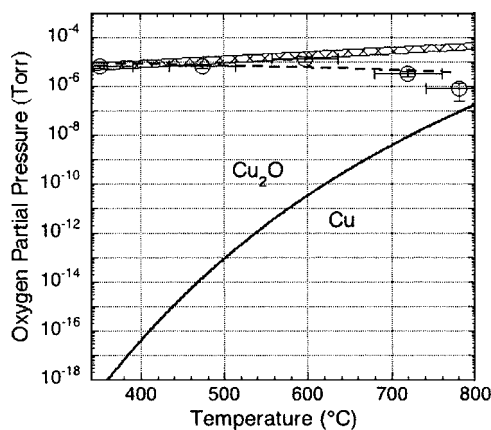


FIG. 3. $p\text{O}_2$ for equilibrium between Cu_2O nanoislands and the Cu (001) surface (open symbols and dashed line drawn as a guide to the eye) was determined to be several orders of magnitude larger than the bulk phase boundary (solid line) and also was found to exhibit much less temperature dependence. Interestingly the narrow window of $p\text{O}_2$ -temperature conditions for which Lyubinetzky *et al.* (Ref. 13) found that single phase Cu_2O nanoclusters could be grown (shown as a cross-hatched region on the phase diagram) is very similar to the phase boundary determined in the present study.

Cu_2O nanoislands formed on Cu (001) are separated by reconstructed surface regions.⁸ Further details of the formation and stability of this surface structure will be reported elsewhere. The Cu_2O islands were observed to nucleate as single crystals, oriented cube-on-cube with the Cu film (i.e., $[100] \text{Cu} \parallel [100] \text{Cu}_2\text{O}$ and $[001] \text{Cu} \parallel [001] \text{Cu}_2\text{O}$). Thus, wide in-plane scans along the $[H00]$ -direction intersect (H00)-type peaks for Cu, Cu_2O , and the SrTiO_3 substrate. Figure 1 shows portions of such scans at 475°C and three different values of $p\text{O}_2$.

Cu– Cu_2O phase equilibria were determined by first nucleating Cu_2O nanoislands, typically at $p\text{O}_2 = 5 \times 10^{-4}$ Torr, and then varying the $p\text{O}_2$ while repeatedly scanning across the Cu_2O (200) reflection. As seen in Fig. 2(a), under conditions where Cu_2O was stable, the oxide Bragg reflection increased in intensity with time, while under conditions where Cu was the stable phase, the Cu_2O (200) reflection continuously weakened, disappearing completely if sufficient time was allowed. Conditions could also be determined for which Cu_2O reflections exhibited constant intensity with time, indicative of a combination of temperature and $p\text{O}_2$ at which Cu and Cu_2O were in thermodynamic equilibrium. As seen in Fig. 2(b), oxidation/reduction conditions were determined at several values of $p\text{O}_2$ at five temperatures from ~ 350 to 780°C . The Cu– Cu_2O phase diagram determined from these measurements (Fig. 3) reveals a striking difference in behavior compared to the bulk phase diagram,⁹ with the Cu– Cu_2O phase boundary shifted several orders-of-magnitude upwards in $p\text{O}_2$, particularly at lower temperatures, and exhibiting very little temperature dependence.

Three possible explanations for the significant change in the phase diagram have been considered: (1) kinetic hindrance, due to the presence of the $c(2 \times 2)$ ordered surface structure; (2) substrate-induced strain, due to the fact that the (001) Cu samples were thin films attached to a SrTiO_3 substrate; and (3) a nanoscale size effect. As discussed below, the third explanation is consistent with our observations, while the first two hypotheses are not.

Qualitatively similar to our observations, Lundgren *et al.*¹⁰ recently found, also via *in situ* x-ray diffraction, that nucleation and growth of PdO on (001) Pd required significantly larger pO_2 than predicted by bulk thermodynamics. They also observed the formation of an oxygen-induced ordered surface structure prior to oxide nucleation¹¹ and interpreted their data as indicating that the surface structure creates a kinetic hindrance to oxide formation by impeding the necessary atomic motions that accompany the phase change. Our data for Cu/Cu₂O phase equilibria, however, are inconsistent with a kinetic hindrance explanation. If the large shift in the phase boundary we observe was due to kinetic hindrance, subsequent reduction of the oxide would still occur at or below the bulk phase boundary, since there should be no kinetic hindrance to reduction (and there would be a large pO_2 difference between conditions for oxidation and reduction). In fact, we observe that reduction occurs at much larger pO_2 than for bulk behavior, and the transition from oxidation to reduction in the case of Cu/Cu₂O requires very small changes in pO_2 . Since reversibility between oxidizing and reducing behavior was not addressed in the report by Lundgren *et al.*,¹⁰ further study of the oxidation behavior of Pd is required to determine whether the early-stage oxidation behavior of the (001) surfaces of these two fcc metals are fundamentally different. For example, differences in the nature of the ordered surface structure for the two materials could be important.

The current data also demonstrate that the shift in the Cu–Cu₂O phase boundary is not caused by substrate-induced constraint of the Cu lattice. Observations of different samples have revealed no film-thickness dependence of the phase boundary. More importantly, we invariably observe normal bulk thermal expansion of the Cu films, indicating that they are fully relaxed.

Our current hypothesis is that the observed behavior is due to the extremely small size of the oxide nanoislands. Both *in situ* x-ray peak broadening measurements and post-mortem *ex situ* AFM observations have revealed that the average size of the noncoalesced Cu₂O islands produced under the range of conditions used in this study is ≤ 30 nm in lateral extent and ≤ 5 nm in height. The limited height of the islands indicates that a large fraction of their atoms are located in close proximity to a surface (i.e., in nonbulk environments where changes in thermodynamic properties would be expected¹²). Since the oxide islands are known to initially grow much more rapidly laterally than in thickness,² our expectation is that Cu–Cu₂O phase equilibria will be relatively insensitive to size until the onset of island coalescence occurs, when increased oxide thickness will result in a significantly smaller fraction of surface atoms.

In addition to providing insight into the initial oxidation of a Cu surface, the observations described here are also relevant to understanding the unusual deposition behavior of oxide nanoparticles or quantum dots. Lyubinetsky *et al.*¹³ recently observed that MBE growth of single-phase Cu₂O

nanoclusters could only be accomplished at several orders-of-magnitude larger pO_2 than the bulk Cu–Cu₂O phase boundary (at higher pO_2 mixed phase Cu₂O–CuO nanoparticles grew, while at lower pO_2 Cu–Cu₂O phase mixtures occurred). As seen in Fig. 3, a comparison of the conditions under which single-phase Cu₂O nanoparticles could be grown by MBE with the phase boundary determined in this study reveals a remarkable similarity, indicating that the small size of nanoclusters results in the formation of equilibrium phases even under MBE growth conditions.

In conclusion, the present study has demonstrated that *in situ* x-ray scattering techniques enable characterization of early-stage oxidation behavior. The very large shift observed in the equilibrium boundary between Cu and Cu₂O phases is believed due to a size-dependent change in thermodynamic properties. Future study is required to determine whether similar behavior occurs for other materials and other surfaces of Cu.

The authors thank the APS Sector 12 (BESSRC) staff for their assistance. Argonne National Laboratory's work was supported by the U.S. Department of Energy, Office of Science, Office of Basic Energy Sciences, under Contract No. W-31-109-Eng-38.

¹N. Cabrera and N. F. Mott, Rep. Prog. Phys. **12**, 163 (1948).

²J. C. Yang, M. Yeadon, B. Kolasa, and J. M. Gibson, Appl. Phys. Lett. **70**, 3522 (1997).

³D. F. Mitchell and M. J. Graham, Surf. Sci. **114**, 546 (1982); L. W. Hobbs and T. E. Mitchell, in *High Temperature Corrosion*, edited by R. A. Rapp (NACE, San Diego, 1981), Vol. 6, pp. 76–83; K. Shimizu, A. Gotoh, K. Kobayashi, G. E. Thompson, and G. C. Wood, in *Microscopy of Oxidation*, edited by M. J. Bennett and G. W. Lorimer (The Institute of Metals, Cambridge University, 1990), Vol. 1, pp. 144–148; R. H. Milne and A. Howie, Philos. Mag. A **49**, 665 (1984).

⁴J. W. Freeland, D. J. Keavney, R. Winarski, P. Ryan, J. M. Slaughter, R. W. Dave, and J. Janesky, Phys. Rev. B **67**, 134411 (2003).

⁵W. Fan, B. Kabius, J. M. Hiller, S. Saha, J. A. Carlisle, O. Auciello, R. P. H. Chang, and R. Ramesh, J. Appl. Phys. **94**, 6192 (2003).

⁶G. W. Zhou and J. C. Yang, Appl. Surf. Sci. **210**, 165 (2003); G. W. Zhou and J. C. Yang, Phys. Rev. Lett. **89**, 106101 (2002); J. C. Yang, D. Evan, and L. Tropa, Appl. Phys. Lett. **81**, 241 (2002); J. C. Yang, M. Yeadon, B. Kolasa, and J. M. Gibson, Scr. Mater. **38**, 1237 (1998); J. C. Yang, B. Kolasa, J. M. Gibson, and M. Yeadon, Appl. Phys. Lett. **73**, 2481 (1998).

⁷G.-W. Zhou and J. C. Yang, Appl. Surf. Sci. **222**, 357 (2004); G.-W. Zhou and J. C. Yang, Surf. Sci. **531**, 359 (2003); **559**, 100 (2004).

⁸J. C. Yang, M. D. Bharadwaj, G. Zhou, and L. Tropa, Microsc. Microanal. **7**, 486 (2001).

⁹R. D. Schmidt-Whitley, M. Martinez-Clemente, and A. Revcolevschi, J. Cryst. Growth **23**, 113 (1974); D. R. Gaskell, *Introduction to Metallurgical Thermodynamics* (Scripta, Washington, D.C., 1973).

¹⁰E. Lundgren, J. Gustafson, A. Mikkelsen, J. N. Andersen, A. Stierle, H. Dosch, M. Todorova, J. Rogal, K. Reuter, and M. Scheffler, Phys. Rev. Lett. **92**, 046101 (2004).

¹¹ $(\sqrt{5} \times \sqrt{5})R27^\circ$ surface reconstruction forms when a clean surface of (001) Pd is exposed to oxygen (see Ref. 10).

¹²B. Krishnamachari, J. McLean, B. Cooper, and J. Sethna, Phys. Rev. B **54**, 8899 (1996).

¹³I. Lyubinetsky, S. Thevuthasan, D. E. McCready, and D. R. Baer, Jpn. J. Appl. Phys., Part 1 **44**, 7926 (2003).